Vortex Glass and Lattice Melting Transitions in a YNi$_2$B$_2$C Single Crystal

Mi-Ock Mun and Sung-Ik Lee

Department of Physics, Pohang University of Science and Technology, Pohang 790-784, Korea

W. C. Lee

Department of Physics, Sookmyung Women's University, Seoul 140-742, Korea

P. C. Canfield, B. K. Cho, and D. C. Johnston

Ames Laboratory, Department of Physics and Astronomy, Iowa State University, Ames, Iowa 50011-3020

The mixed state of the weakly disordered superconductor YNi$_2$B$_2$C is found to be similar to that of high-T_c materials due to its large fluctuations. The very sharp resistive transition with a kink and the S-shaped I-V curve appear below $H = 1$ T indicating a lattice melting transition. The scaling behavior of the vortex glass transition in R-T and I-V curves for $H \geq 2$ T is observed with critical exponents $\nu = 1.23 \pm 0.02$ and $z = 5.46 \pm 0.32$, which are field independent. The vortex solid state changes from the vortex lattice at low fields to the vortex glass at high fields due to a field-enhanced pinning effect. The type of multicriticality is not yet conclusive.

It has been shown that the mixed state is no longer the simple Abrikosov flux lattice phase in high-T_c cuprate superconductors [1–8]; this is because of the large fluctuations originating from the high transition temperature and the short coherence length. This fluctuation effect is enhanced by the low dimensionality resulting from the layered structure and the high anisotropy. The mixed state separates into two different states, i.e., a real superconducting vortex solid and a resistive vortex liquid. The vortex solid state can be vortex lattice or vortex glass depending on the disorder of a system. The newly discovered intermetallic type-II superconductor YNi$_2$B$_2$C [9], on the other hand, has a low transition temperature and a relatively large coherence length; it is a nearly isotropic three-dimensional superconductor [10–12] in spite of its layered structure with stacking sequence ((B-Ni$_2$-B-YC)$_n$ [13,14]. Nevertheless, we found that thermal fluctuations of this system are larger than those of conventional low-T_c superconductors. The Ginzburg number $G_i = (1/2)[T_c/H_c^2(0)\gamma\xi_0^3]^2$, which represents the order of thermal fluctuations, is $\sim 10^{-7}$ for YNi$_2$B$_2$C, while it is $\sim 10^{-9}$ for conventional superconductors and $\sim 10^{-5}$ for high-T_c materials. Therefore, the vortex states of YNi$_2$B$_2$C can be quite unusual compared to conventional superconductors. Moreover, the low value of the upper critical field makes it possible to study the overall H-T phase diagram down to low temperature regimes not possible in high-T_c copper oxides.

In this study, we found that YNi$_2$B$_2$C shows a sudden drop with a kink feature in the superconducting transition region and an S-shaped I-V curve for fields below 1 T. This is a sign of the first order lattice melting transition as found in clean high-T_c materials [7,8]. We also found that the vortex melting obeys the prediction of the elasticity theory based on the Lindemann criterion [15,16]. The quantum fluctuation effect is relatively minor compared to thermal fluctuations. For $H \geq 2$ T, the scaling behavior in both R-T and I-V curves fulfills the vortex glass transition theory with the field-independent critical exponents of $\nu = 1.23 \pm 0.02$ and $z = 5.46 \pm 0.32$. These exponents are consistent with theory [17,18] as well as experimental results in high-T_c materials [1–3]. The second order vortex glass transition line is well described by the theoretical prediction [17] of $H_g \sim (T_c - T)^{4/3}$.

The single crystal YNi$_2$B$_2$C was grown by the high temperature flux method using Ni$_2$B as a solvent. The details are described in Ref. [19]. The crystal is plate-like and its physical dimension is about $1.2 \times 0.7 \times 0.025$ mm^3. The external magnetic field was applied parallel to the c axis and perpendicular to the current direction. The zero-field resistivity is $\rho \sim 1.05$ $\mu\Omega$ cm just above the transition temperature, the zero-field transition temperature $T_c(0)$ is 15.7 K, and the transition width is less than 100 mK.

The magnetic field dependent resistance of the YNi$_2$B$_2$C single crystal seemed to show typical behavior as a conventional superconductor [19,20]. The details of the transition, however, depend on the field strength (Fig. 1), and this is related to the nature of the vortex states.

For $H \leq 1$ T in Fig. 1, the resistance decreases very sharply with $\Delta T_m/T_c \sim 10^{-3}$ and shows a kink feature at $R/R_n \sim 0.1$, which is claimed to be one of the indications for vortex lattice melting transition [7,8]. The I-V characteristics of $H \leq 1$ T show the pronounced feature supporting the lattice melting [6,7]. At $H = 0.5$ T (Fig. 2), the linearity of the I-V curve starts to be shown at $T_m = 13.60$ K, the melting temperature. A slightly S-shaped nonlinear behavior is also observed at $T = 13.50$ K in the region of $T_{c,\text{zero}} < T < T_m$, which
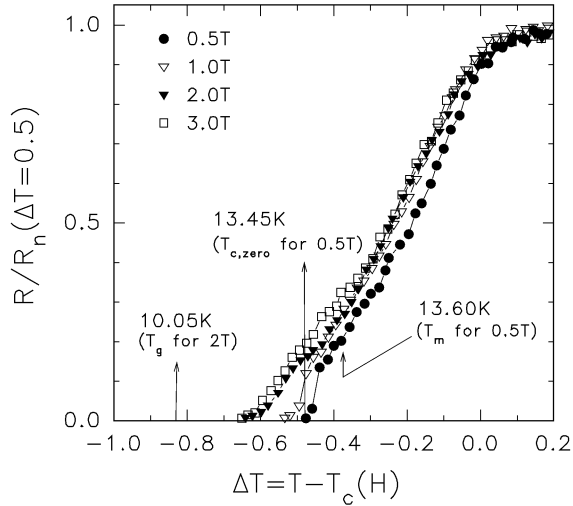
FIG. 1. At fields below 1 T, the curves show an abrupt drop with the kink feature in the transition region. For fields above 2 T, the resistive transitions are continuous. The field-dependent transition temperatures $T_c(H)$ are 13.92 K (0.5 T), 12.78 K (1.0 T), 10.84 K (2.0 T) and 9.22 K (3.0 T).

corresponds to the kink regime of the R-T curve as represented by arrows in Fig. 1. The lattice melting line $B_m(T)$ is calculated using nonlocal elasticity theory based on the Lindemann criterion, including thermal fluctuations [15] and quantum fluctuations [21,22] as

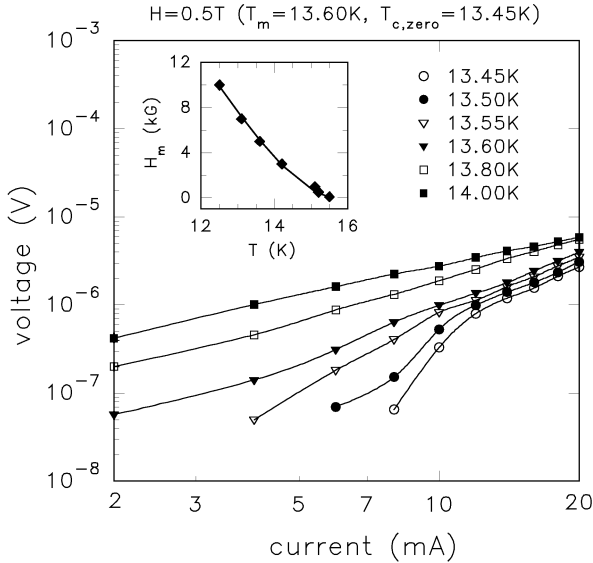$$B_m(T) \approx H_{c2}(0)\frac{4\theta^2}{(1 + \sqrt{1 + 4S\theta T_c/T})^2}, \qquad (1)$$

FIG. 2. I-V curves at $H = 0.5$ T at corresponding temperatures indicated in Fig 1. An Ohmic behavior in the I-V curve starts to appear at $T = 13.60$ K, the melting temperature. There appears a slightly S-shaped curve in the kink region of the $R - T$ curve. Inset: The vortex lattice melting line of YNi$_2$B$_2$C below 1 T. The solid line is the fitting result by Eq. (1).

with

$$\theta = c_L^2 \sqrt{\beta_m/G_i}\left(\frac{T_c}{T} - 1\right),$$

$$S = q + c_L^2 \left(\frac{\beta_m}{G_i}\right)^{1/2},$$

with c_L the Lindemann criterion and a constant $\beta_m \approx 5.6$. The quantum parameter q is defined as $q \approx 2.4\nu_q/K_F\xi$ with ν_q the cutoff frequency due to an energy gap, K_F the Fermi wave vector, and ξ the coherence length. The physical quantities of YNi$_2$B$_2$C are $G_i = 3.22 \times 10^{-7}$, $c_L = 0.02$, $H_{c2} = 8$ T, $T_c = 15.7$ K, $\gamma = 0.8$, and the Ginzburg-Landau parameter is $\kappa = 18$ [23]. The experimental melting line follows Eq. (1) with a single fitting parameter $q = 0.25$ (inset of Fig. 2), and so the quantum contribution to the lattice melting is minor compared to the thermal effects. The melting field is described with a simple power law of $H_m \sim (T_c - T)^\alpha$ with $\alpha = 1.61$, which is compatible with the theoretical calculation. Considering the limiting behavior of Eq. (1),

$$B_m \approx \begin{cases} H_{c2}(0)\theta^2, & \theta \to 0 \\ \theta T/ST_c, & \theta > 1/S, \end{cases} \qquad (2)$$

we can see that as the field increases or the temperature decreases the effective power for the melting line becomes smaller than 2 which is the power near T_c. The value of the Lindemann criterion $c_L = 0.02$ is much smaller than $c_L = 0.1-0.4$ for highly anisotropic high-T_c superconductors [15]. Brandt [16] proved that the smaller value of c_L ($\approx 1/20$) is more realistic by calculating the fluctuating shear strain from the nonlocal elasticity of the vortex lattice. A recent Monte Carlo simulation [24] also showed that c_L decreases when the vortex lattice changes from a 2D structure to a fragile 3D lattice. This was also confirmed experimentally for Nb films with $\kappa = 10.8$, in which c_L was 0.04 [25].

When $H \gtrsim 2$ T (Fig. 1), the R-T curves show a continuous transition. The melting temperature at which the I-V curve becomes linear is above the kink regime as indicated by the arrow in Fig. 1 for $H = 0.5$ T and $T_m = 13.60$ K. However, for the I-V curves of $H = 2$ T, the curvature changes at the glass transition temperature T_g, which is located at temperature below the appearance of the resistive tail as represented by the arrow.

From the assumed Arrhenius form of resistance, $R(T) = R_o \exp(-U_0/k_BT)$, the temperature dependence of an activation energy U_0 (inset of Fig. 3) is calculated as is the single crystal Bi$_2$Sr$_2$CaCu$_2$O$_{8+\delta}$ [3]. U_0 starts to diverge at temperature T^*, below which the vortices are not in the thermally activated region but in the critical regime associated with the phase transition. Assuming a second order vortex glass phase transition [17], the linear resistance in the regime of $T_g < T < T^*$ is analyzed with the scaling form of $R_L \sim (T - T_g)^{\nu(z-1)}$. For $H = 3$ T (Fig. 3), the scaling analysis gives 6.06 for $\nu(z-1)$ using $T_g = 8.37$ K
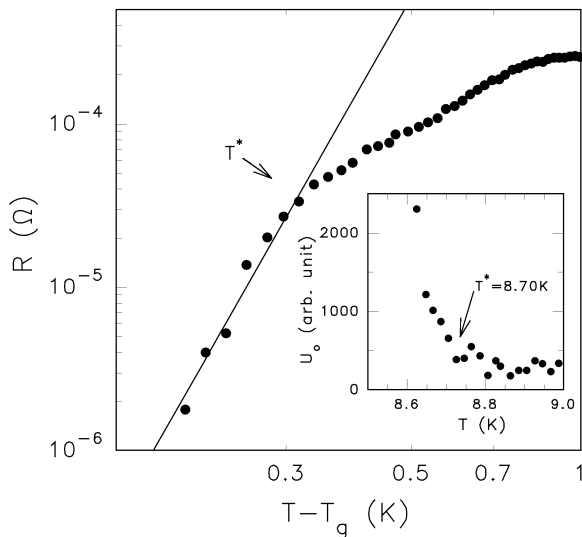
FIG. 3. The linear resistance for a field of 3 T scales with $T_g = 8.37$ K determined in I-V curves and the critical exponent $\nu(z - 1)$ is 6.06. Inset: The activation energy $U_0 = -d(\ln R)/d(T^{-1})$ as a function of temperature. T^* is the temperature at which the activation energy starts to diverge.
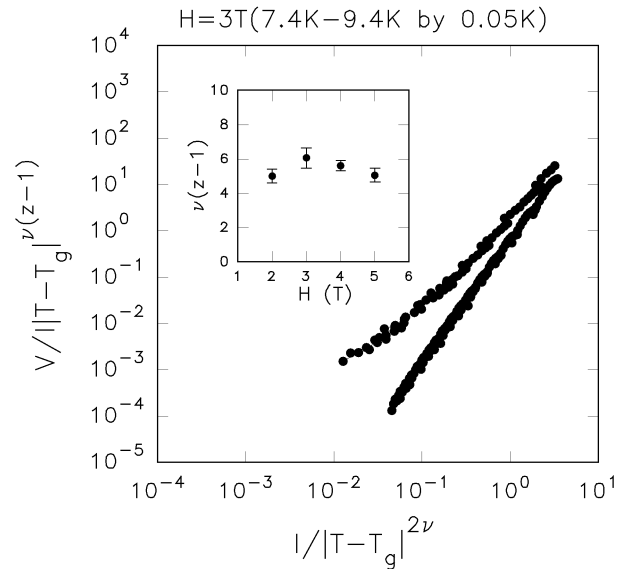

FIG. 4. The scaling of voltage-current curves of $H = 3$ T at temperatures from 7.4 K to 9.4 K by 0.05 K. The critical exponents are $\nu = 1.25$ and $z = 5.86$, which are consistent with the result of the R-T curve scaling. Inset: The critical exponent $\nu(z - 1)$ for various fields above 2 T.

determined from the I-V curves. As shown in Fig. 4, the I-V curves of $H = 3$ T are also scaled with

$$E(J) \approx J\xi^{d-2-z}\bar{E}_\pm(J\xi^{d-1}\phi_o/k_BT) \qquad (3)$$

near the glass transition temperature T_g. The resulting values of $\nu = 1.25$ and $z = 5.85$ are consistent with the R-T scaling when $d = 3$. From analysis for fields above 2 T, the critical exponents $\nu = 1.23 \pm 0.02$ and $z = 5.46 \pm 0.32$ are found to be field independent (inset of Fig. 4) within the theoretically expected values of $z > 4$ and $1 < \nu < 2$ [17,18]. The vortex glass transition line $H_g(T)$ is consistent with the theoretical prediction [17] $H_g(T) \sim (T_c - T)^{4/3}$ (dashed line in Fig. 5), which is different from the lattice melting line $H_m(T) \sim (T_c - T)^{1.61}$.

The H-T phase diagram of YNi$_2$B$_2$C (Fig. 5) shows the first order lattice melting transition at low fields and the second order vortex glass phase transition at high fields. Both the vortex lattice and the vortex glass phases appear for one sample due to the field-dependent effects of disorder. In a weakly disordered system, vortices sustain the lattice structure at low fields [5]. As the field increases, however, the effective pinning strength of the disorder increases [17] and the vortex lattice becomes no longer stable and forms a vortex glass. For the untwinned YBa$_2$Cu$_3$O$_y$ single crystal [5], similar multicritical behavior was observed and it was shown that the critical end point of the second order phase transition occurs in the middle of the first order transition line. However, the type of multicriticality in the YNi$_2$B$_2$C single crystal is not yet conclusive in the crossover region of 1 T $\leq H \leq 2$ T and 10 K $\leq T \leq 12$ K.

In conclusion, our measurements are consistent with the vortex lattice melting transition at low fields and

the vortex glass transition at high fields in the YNi$_2$B$_2$C single crystal. This phase change, depending on magnetic field, is possible in weakly disordered systems because the field-enhanced disorder transforms the system from the vortex lattice phase into the vortex glass phase. Because the vortex lattice is robust with respect to the weak pinning, the resistance decreases suddenly with a
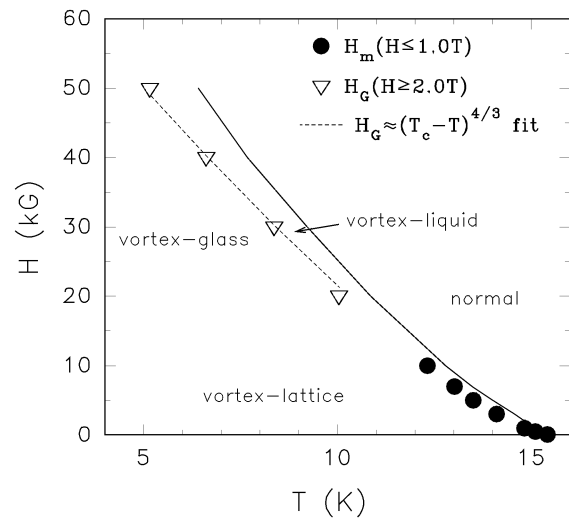

FIG. 5. The H-T phase diagram of YNi$_2$B$_2$C single crystal obtained from the transport measurement. There are both the vortex lattice melting transition and the vortex glass transition due to the field-enhanced effect of the disorder in the weakly disordered system. (Solid line, field-dependent superconducting onset temperature; filled circle, H_m; hollow triangle, H_g; and dotted line, the theoretically expected line for glass transition).

kink feature in the R-T curve and an S-shaped nonlinear I-V curve appears below T_m indicating the first order transition for $H \leq 1$ T. When the field increases above 2 T, the continuous vortex glass transition is observed with self-consistent scaling behaviors in the R-T and the I-V curves. Although the vortex liquid regime is very narrow compared to high-T_c superconductors due to the low transition temperature and the 3D superconductivity, the mixed state properties of the YNi_2B_2C superconductor are found to be similar to those of high-T_c cuprates.

[1] R. H. Koch, V. Foglietti, W. J. Gallagher, G. Koren, A. Gupta, and M. P. A. Fisher, Phys. Rev. Lett. **63**, 1511 (1989).

[2] P. L. Gammel, L. F. Schneemeyer, and D. J. Bishop, Phys. Rev. Lett. **66**, 953 (1991).

[3] H. Safar, P. L. Gammel, D. J. Bishop, D. B. Mitzi, and A. Kapitulik, Phys. Rev. Lett. **68**, 2672 (1992).

[4] H. Safar, P. L. Gammel, D. A. Huse, D. J. Bishop, J. P. Rice, and D. M. Ginsberg, Phys. Rev. Lett. **69**, 824 (1992).

[5] H. Safar, P. L. Gammel, D. A. Huse, D. J. Bishop, W. C. Lee, J. Giapintzakis, and D. M. Ginsberg, Phys. Rev. Lett. **70**, 3800 (1993).

[6] W. K. Kwok, J. Fendrich, U. Welp, S. Fleshler, J. Downey, and G. W. Crabtree, Phys. Rev. Lett. **72**, 1088 (1994).

[7] W. K. Kwok, J. Fendrich, S. Fleshler, U. Welp, J. Downey, and G. W. Crabtree, Phys. Rev. Lett. **72**, 1092 (1994).

[8] W. K. Kwok, S. Fleshler, U. Welp, V. M. Vinokur, J. Downey, and G. W. Crabtree, Phys. Rev. Lett. **69**, 3370 (1992).

[9] R. J. Cava, H. Takagi, H. W. Zandbergen, J. J. Krajewski, W. F. Peck, Jr., T. Siegrist, B. Batlogg, R. B. van Dover, R. J. Felder, K. Mizuhashi, J. O. Lee, H. Eisaki, and S. Uchida, Nature (London) **367**, 252 (1994).

[10] N. M. Hong, H. Michor, M. Vybornov, T. Holubar, P. Hundegger, W. Pethold, G. Hilscher, and P. Rogl, Physica (Amsterdam) **227C**, 85 (1994).

[11] Y. Y. Xue, Y. Cao, R. L. Meng, C. Kinalidis, and C. W. Chu, Physica (Amsterdam) **227C**, 63 (1994).

[12] E. Pickett and D. J. Singh, Phys. Rev. Lett. **72**, 3702 (1994).

[13] T. Siegrist, H. W. Zandbergen, R. J. Cava, J. J. Krajewski, and W. F. Peck, Jr., Nature (London) **367**, 254 (1994).

[14] B. C. Chakoumakos and M. Paranthaman, Physica (Amsterdam) **227C**, 143 (1994).

[15] A. Houghton, R. A. Pelcovits, and A. Sudbø, Phys. Rev. B **40**, 6763 (1989).

[16] E. H. Brandt, Phys. Rev. Lett. **63**, 1106 (1989).

[17] D. S. Fisher, M. P. A. Fisher, and D. A. Huse, Phys. Rev. B **43**, 130 (1991).

[18] A. Houghton and M. A. Moore, Phys. Rev. B **38**, 5045 (1988).

[19] M. Xu, P. C. Canfield, J. E. Ostenson, D. K. Finnemore, B. K. Cho, Z. R. Wang, and D. C. Johnston, Physica (Amsterdam) **227C**, 321 (1994).

[20] H. Tagaki, R. J. Cava, H. Eisaki, J. O. Lee, K. Mizuhashi, B. Batlogg, S. Uchida, J. J. Krajewski, and W. F. Peck, Jr., Physica (Amsterdam) **228C**, 389 (1994).

[21] G. Blatter and B. I. Ivlev, Phys. Rev. Lett. **70**, 2621 (1993).

[22] G. Blatter and B. I. Ivlev, Phys. Rev. B **50**, 10 272 (1994).

[23] M. S. Kim *et al.* (unpublished).

[24] S. Ryu, S. Doniach, G. Deutscher, and A. Kapitulnik, Phys. Rev. Lett. **68**, 710 (1992).

[25] M. F. Schmidt, N. E. Israeloff, and A. M. Goldman, Phys. Rev. Lett. **70**, 2162 (1993).